In situ chemical probing of the electrode-electrolyte interface by ToF-SIMS

Bingwen Liu,[a] Xiao-Ying Yu,*[a] Zihua Zhu,*[b] Xin Hua,[a] Li Yang,[b] and Zhaoying Wang[b]

[a] *Atmospheric Sciences and Global Climate Change Division, Pacific Northwest National Laboratory, Richland, WA 99354, USA, E-mail: xiaoying.yu@pnnl.gov*
[b] *Scientific Resources Division, W.R. Wiley Environmental Molecular Science Laboratory, Pacific Northwest National Laboratory, Richland, WA 99354, USA, E-mail: zihua.zhu@pnnl.gov*

Experimental Details

Here we present technical details describing device fabrications, device dimensions, components, and equipment.

The photomask was designed using the AutoCAD software and printed with a mask printer (Intelligent Micro Patterning LLC, Model SF-100 Xpress). First, a template for casting was made on a silicon substrate, with SU-8 photoresist (Microchem, Newton, MA). The template has features about 300 μm deep which defines the depth of the EC cell, that is, the distance between the working electrode and the counter electrode (see Fig. 1(a)). The dimension of the EC cell is approximately 2.5×2.5×0.3 mm^3.

A 10:1 ratio (w/w) of polydimethylsiloxane (PDMS) prepolymer and curing agent (Sylgard 184, Dow Corning Co., Midland, MI, USA) were thoroughly mixed, degassed under vacuum, poured onto the patterned template to a thickness of 1 cm, and cured in an oven at 75 °C overnight.[1, 2] The counter electrode was made of Pt. High temperature epoxy (Duralco 4461, Cotronics Co., Brooklyn, NY) was used to form the base block for hosting the wires to connect the Pt electrodes and the external electrochemical work station. It was fabricated by inserting the copper metal wires (diameter 600 μm for the counter electrode and 350 μm for the reference electrode, respectively) through a PDMS block. Once the wires were secured in the block, a mixture of epoxy was poured and cured for 24 hrs at room temperature followed by 2 hrs heating at 110 °C in the oven. The surface of the epoxy block with embedded wires was polished with fine sand papers to create a flat surface for sputter coating of Pt forming the metal electrode. Prior to Pt sputtering (Denton Vacuum, LLC, Moorestown, NJ), the two electrodes were separated by a narrow strip of tape (Fig. 1(b)). The Pt target was acquired from Kurt J. Lesker Co., Clariton, PA with a purity of 99.99%. The sputtered Pt electrode is 200 nm thick. The tape was removed after sputter coating forming the counter electrode and reference electrode. The dimension of the Pt counter electrode is ~ 2.3×3 mm^2, and the Pt reference electrode is ~ 0.5×3 mm^2.

The epoxy block was placed onto a SU-8 template containing the inlet and outlet ports for electrolyte solutions and PDMS was cast. After removing the patterned PDMS substrate from the template, two 0.5 mm diameter through-holes was made at the end of the round reservoir by punching the substrate with a sharpened flat syringe needle (NE-301PL-C; Small

Parts, Miramar, FL). The Au electrode was sputter coated (Model 30800, Ladd Research Industries Inc., Burlington, VT) on the backside of the silicon nitride (SiN) membrane (window: 100 nm thickness SiN membrane, 1.5×1.5 mm^2; and frame: 200 μm thickness silicon, 7.5×7.5 mm^2, Norcada Inc., Canada) with a thickness of 20 nm (Fig 1(c)). The dimension of the Au electrode is ~ 2 ×2 mm^2. Here we simply assume that the actual electrode surface area is equal to the geometric area. The PDMS piece and the SiN piece were treated with oxygen plasma before bonding. The flow reservoir and microchannels were enclosed by irreversibly bonding the PDMS block and the SiN window.

The EC vacuum interface consists of a PDMS microfluidic block, electro-osmotic pump (Model: 3000126, Dolomite, United Kingdom, battery (Saft, Li-$SOCl_2$), and PTFE connecting tubings (Valco Instruments Co. Inc. TX). The PDMS microfluidic block except for the membrane window was coated by a thin layer of gold film. The continuous flow in the channel was obtained by an electro-osmotic pump adapted for vacuum compatibility and it was powered by a hermetic, glass-metal-sealed 3.6 V thionyl chloride lithium batteries (SAFT 1/2 AA, LS-14250).[5, 6] It is used to reduce beam damage and keep stable electrolyte supply. The wire connections were covered by UHV compatible fiberglass sleeving. A short capillary (Polymicro Technologies, 360 μm OD and 74 μm ID) was inserted in the PTFE tubing to form a tee. Above the channel and reservoir on the SiN window, a hole of approximately 2 μm in diameter was drilled through by the ToF-SIMS primary ion beam.

Additional Figures

Figure S-1 depicts the ToF-SIMS depth profiling time series illustrating the drill through of the SiN membrane, the gold electrode coated on the backside of the SiN, and observations of the electrolyte adjacent to the electrode. During drilling, a Bi^+ beam (pulse width = 1000 ns) with 20 kHz repeating rate was used. At sputter time 40 s, the SiN membrane and Au film electrode were drilled through. This was confirmed by the sharp increase of the intensity of H^- and O^- signals, indicating that the electrolyte surface is being seen. After 2-3 more seconds (at 42-43 s), the Bi^+ beam pulse was changed from 1000 ns to 200 ns for better mass resolution so that peak assignment was possible. It should be mentioned that with 1000 ns pulse, only H^- and O^- signals can be easily separated from interferences.

It is interesting to note that signals of species that are known to form as a result of subsequent interfacial reactions, such as AuI_2^-, I_2^-, and I_3^-, can be detected after about 45 s. Their signal intensities rise quickly and then reduce sharply. Species that are known to form as a result of the redox reactions at higher potential in the electrolyte, such as IO_3^-, also were observed. However, the IO_3^- signal decreases dramatically with time, indicating that the rate for it to form (or disappear) is slower, because it is one of the more oxidized products (see reaction (4)) in the chain reactions.

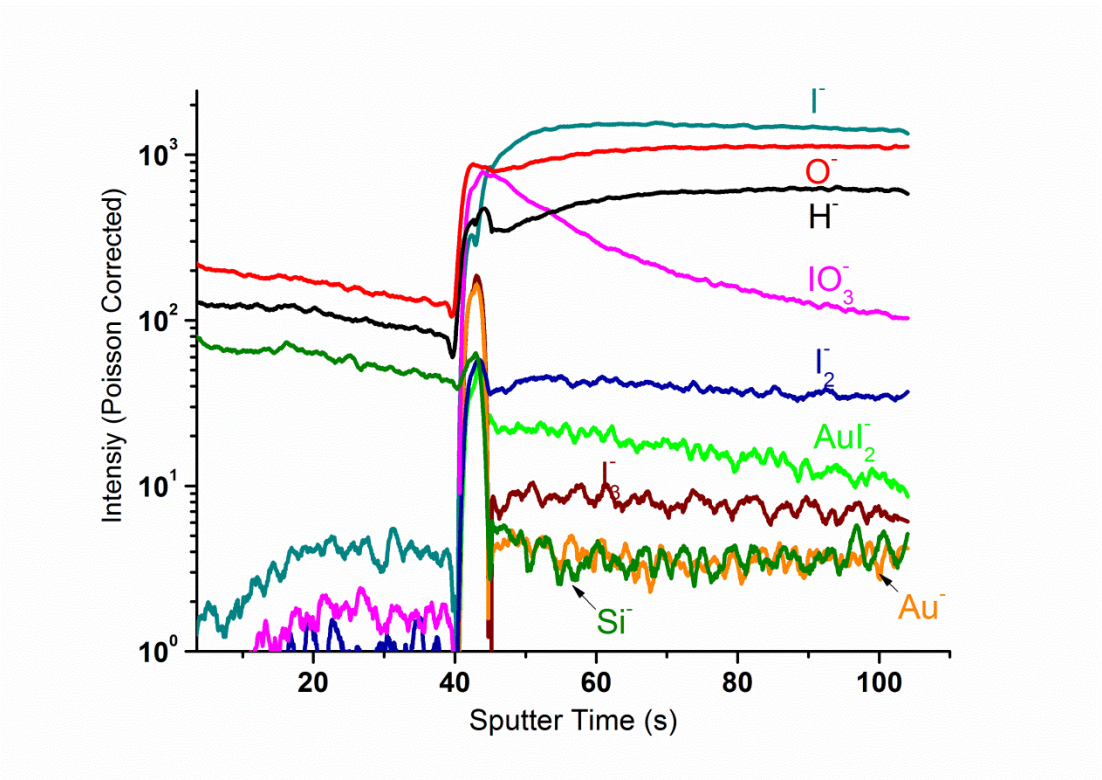

Figure S-1. The ToF-SIMS depth profiling time series illustrating direct observations of the electrode-electrolyte interface.

Each curve in **Figure S-1** (45 s to 100 s range) corresponds to a 2D image of individual species shown in **Figure 3** and each image within **Figure 3** corresponds to a m/z peak shown in **Figure 2**. These experimental data are strong evidences that the depth profiling mode provides direct spatial measurements of the electrode-electrolyte interface.

For better understanding, we drew a schematic illustration (Figure S-2) to show aperture evolution:

Figure S-2 A corresponds to about the 10 s sputtering time in Figure S-1. Some SiN material was sputtered away. Figure S-2 B corresponds to the ~38 s in Figure S-1. Some Au was sputtered away, but no liquid was detected. Figure S-2 C corresponds to the ~45 s in Figure S-1. The Bi^+ has sputtered through the Au layer; however, the aperture size was small. Figure S-2 D corresponds to the ~100 s in Figure S-1. The aperture became larger with more Bi^+ sputtering.

The electrode/electrolyte interface may be a ring (see red arrows in Figure S-2 C). This interface is highly dynamic because high Bi^+ current density was used in our measurements. Thus, the aperture became larger and larger during measurements. Meanwhile, excellent detection limit of SIMS ensured us to get signals of interest, such as AuI_2^- and I_2^-, from this interface, although the area was limited.

We may detect electrochemical products from electrolyte/vacuum interface also, because soluble species of interest, such as IO_3^- and I_3^-, can diffuse from the adjacent Au/electrolyte interface.

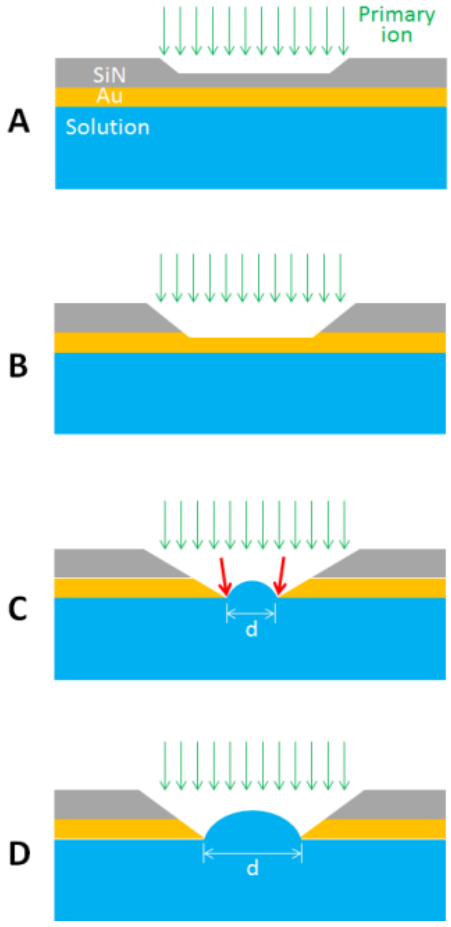

Figure S-2. A schematic illustration of the aperture evolution during ToF-SIMS measurement.

Figure 2(b) depicts the m/z spectrum obtained at 0.8 V by the ToF-SIMS; however, only peaks of interest are shown. An example of complete m/z spectra obtained at different potentials is provided below in Figure S-3.

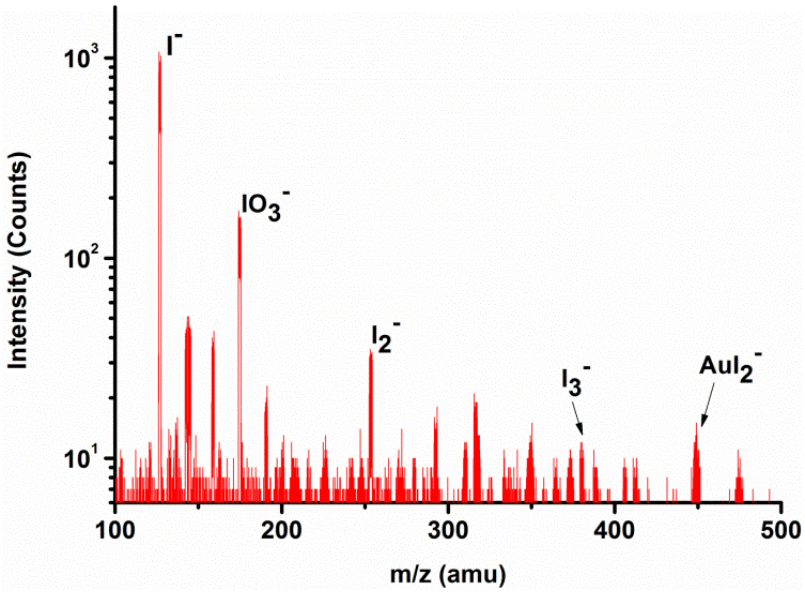

Figure S-3: The ToF-SIMS m/z spectrum acquired at 0.8 V.

Additional References

The following references are not included due to the space constraint of the manuscript. They are provided for the convenience of readers for further investigations and discussions.

EC cells developed for synchrotron studies are also provided.[3-12] However, these existing cells do not employ microfluidic approach.

Additional papers describing the study of the KI electrolyte in a three electrode system are included for the interest of readers.[13-23]

References

1. T. Yamada, N. Batina and K. Itaya, *Surf. Sci.*, 1995, **335**, 204-209.
2. T. Yamada, N. Batina and K. Itaya, *Journal of Physical Chemistry*, 1995, **99**, 8817-8823.
3. M. Balasubramanian, X. Sun, X. Q. Yang and J. McBreen, *Journal of Power Sources*, 2001, **92**, 1-8.
4. M. G. Dowsett and A. Adriaens, *Anal. Chem.*, 2006, **78**, 3360-3365.
5. M. L. Foresti, A. Pozzi, M. Innocenti, G. Pezzatini, F. Loglio, E. Salvietti, A. Giusti, F. D'Anca, R. Felici and F. Borgatti, *Electrochim. Acta*, 2006, **51**, 5532-5539.
6. J. B. Leriche, S. Hamelet, J. Shu, M. Morcrette, C. Masquelier, G. Ouvrard, M. Zerrouki, P. Soudan, S. Belin, E. Elkaim and F. Baudelet, *Journal of the Electrochemical Society*, 2010, **157**, A606-A610.
7. G. A. Roberts and K. D. Stewart, *Review of Scientific Instruments*, 2004, **75**, 1251-1254.

8. G. Scherb, A. Kazimirov and J. Zegenhagen, *Review of Scientific Instruments*, 1998, **69**, 512-516.

9. G. Scherb, A. Kazimirov, J. Zegenhagen, T. L. Lee, M. J. Bedzyk, H. Noguchi and K. Uosaki, *Physical Review B*, 1998, **58**, 10800-10805.

10. P. M. A. Sherwood, *Colloids and Surfaces a-Physicochemical and Engineering Aspects*, 1998, **134**, 221-230.

11. S. Warren, T. L. Lee, J. Zegenhagen, A. Reitzle, D. M. Kolb, J. Ziegler, F. Maroun, P. Allongue, A. Kazimirov and G. Scherb, *X-ray structural analysis of semiconductor-electrolyte interfaces*, World Scientific Publ Co Pte Ltd, Singapore, 2003.

12. X.-Q. Yang and K.-W. Nam, unpublished work.

13. J. P. Bellier and A. Hamelin, *Comptes Rendus Hebdomadaires Des Seances De L Academie Des Sciences Serie C*, 1975, **280**, 1489-1492.

14. J. Wang, B. M. Ocko, A. J. Davenport and H. S. Isaacs, *Physical Review B*, 1992, **46**, 10321-10338.

15. B. M. Ocko, G. M. Watson and J. Wang, *Journal of Physical Chemistry*, 1994, **98**, 897-906.

16. X. P. Gao, G. J. Edens, F. C. Liu, A. Hamelin and M. J. Weaver, *Journal of Physical Chemistry*, 1994, **98**, 8086-8095.

17. K. Itaya, *Prog. Surf. Sci.*, 1998, **58**, 121-247.

18. N. J. Tao and S. M. Lindsay, *Journal of Physical Chemistry*, 1992, **96**, 5213-5217.

19. H. W. Lei, H. Uchida and M. Watanabe, *Langmuir*, 1997, **13**, 3523-3528.

20. A. Hightower, B. Koel and T. Felter, *Electrochim. Acta*, 2009, **54**, 1777-1783.

21. A. C. Chen, Z. C. Shi, D. Bizzotto, J. Lipkowski, B. Pettinger and C. Bilger, *J. Electroanal. Chem.*, 1999, **467**, 342-353.

22. N. Y. Gu, L. Niu and S. J. Dong, *Electrochem. Commun.*, 2000, **2**, 48-50.

23. K. Itaya, N. Batina, M. Kunitake, K. Ogaki, Y. G. Kim, L. J. Wan and T. Yamada, in *Solid-Liquid Electrochemical Interfaces*, eds. G. Jerkiewicz, M. P. Soriaga, K. Uosaki and A. Wieckowski, Amer Chemical Soc, Washington, 1997, vol. 656, pp. 171-188.